



The ^{226}Ra enrichment in oceanic basalts: Evidence for melt-cumulate diffusive interaction processes within the oceanic lithosphere

Alberto E. Saal

Department of Geological Sciences, Brown University, 324 Brook Street, Box 1846, Providence, Rhode Island 02912, USA (asaal@brown.edu)

James A. Van Orman

Department of Geological Sciences, Case Western Reserve University, 112 A.W. Smith Building, Cleveland, Ohio 44106, USA (jav12@cwru.edu)

[1] U-Th decay chains in young volcanic rocks have become a unique geochemical tool with the potential to constrain the physical processes involved in the generation and transport of magmas. Among the different isotopes of the decay series, the measured disequilibrium between ^{226}Ra and ^{230}Th isotopes in basaltic melts has been a crucial player in the interpretation of the U-series data as a whole. However, the key assumption proposed in all previous models, that the origin of ^{226}Ra - ^{230}Th disequilibrium in oceanic basalts is only produced during mantle melting processes, has remained largely unchallenged. Here we present an alternative process for the origin of the ^{226}Ra - ^{230}Th disequilibrium in oceanic basalts. We argue that diffusive interaction of magmas with cumulates formed in the oceanic crust beneath mid ocean ridges or oceanic islands may be responsible for the observed ^{226}Ra - ^{230}Th disequilibrium in oceanic basalts. Hence the inferences drawn from $(^{226}\text{Ra})/(^{230}\text{Th})$ activity ratios about mantle melting and melt transport processes beneath mid-ocean ridges and ocean islands are at best equivocal.

Components: 8829 words, 4 figures, 3 tables.

Keywords: U-series; oceanic basalts.

Index Terms: 1040 Geochemistry: Isotopic composition/chemistry; 3035 Marine Geology and Geophysics: Midocean ridge processes; 3640 Mineralogy and Petrology: Igneous petrology.

Received 14 August 2003; **Revised** 5 November 2003; **Accepted** 24 November 2003; **Published** 25 February 2004.

Saal, A. E., and J. A. Van Orman (2004), The ^{226}Ra enrichment in oceanic basalts: Evidence for melt-cumulate diffusive interaction processes within the oceanic lithosphere, *Geochem. Geophys. Geosyst.*, 5, Q02008, doi:10.1029/2003GC000620.

1. Introduction

[2] Understanding the physical processes involved in the generation and transport of magmas is a key problem in igneous petrology. The measurement of radioactive disequilibrium between the short-lived nuclides of the U-Th decay chains in young volcanic rocks has the potential to constrain the

timescales of melting and melt transport and the melt fraction present during melting [McKenzie, 2000]. Consequently, such geochemical measurements may provide quantitative information on key physical parameters involved in melt generation and transport processes. Two main characteristics of these isotopic systems make them unique: (1) all elements involved are highly incompatible, with



bulk partition coefficients ranging from 10^{-3} to 10^{-5} [Blundy and Wood, 2003, and references therein], indicating short residence times in the solid during mantle melting, and (2) they have half-lives comparable to the time required for melt generation and transport, ranging from a few thousand to a few hundred thousand years.

[3] Thus far, ^{238}U - ^{230}Th - ^{226}Ra and ^{235}U - ^{231}Pa isotopic systems have been used in ocean island and mid-ocean ridge basalts to infer mantle upwelling velocities, melting rates, mantle porosity, extent of mantle melting and the current Th/U ratios of the mantle source [Lundstrom, 2003; Bourdon and Sims, 2003, and references therein]. These parameters have been extracted by applying several different melting models to U series disequilibrium measured in basaltic lavas. The simplest is the batch melting model, which assumes that the maximum deviation from secular equilibrium is solely due to chemical fractionation [Allègre and Condomines, 1982; Sims *et al.*, 1995]. The “dynamic melting” model [McKenzie, 1985; Williams and Gill, 1989; McKenzie, 2000] assumes slow, near-fractional melting and instantaneous melt extraction, where the higher solid residence time of the parent relative to the daughter nuclide produces ingrowth and excess daughter nuclide during melting [McKenzie, 1985; Williams and Gill, 1989; McKenzie, 2000]. Finally, there are equilibrium porous flow models where ingrowth of the daughter isotope occurs not only during melting, but also during melt transport processes [Spiegelman and Elliott, 1993; Iwamori, 1994; Lundstrom, 2000; Jull *et al.*, 2002]. The central problem in using those models is that the actual inferences drawn from U series measurements depend significantly on the model used to interpret them [Spiegelman, 2000].

[4] ^{226}Ra - ^{230}Th disequilibrium has been a crucial player in the interpretation of the U-series data, because it limits the number of possible melting models able to explain ^{238}U - ^{230}Th - ^{226}Ra and ^{235}U - ^{231}Pa disequilibrium data. For example, while ^{230}Th - ^{238}U and ^{231}Pa - ^{235}U disequilibrium in Hawaiian lavas can be explained by either simple batch melting or any of the ingrowth models, the ^{226}Ra - ^{230}Th disequilibrium cannot be explained by batch melting and requires models

that explicitly consider the time scale of melt generation and transport, such as dynamic melting or equilibrium porous flow models [Sims *et al.*, 1995, 1999]. Therefore understanding the origin of the ^{226}Ra - ^{230}Th disequilibrium is crucial to the interpretation of U-series disequilibria as a whole. For example, if the ^{226}Ra - ^{230}Th disequilibrium in oceanic basalts is the result of a process different from mantle melting, our ability to distinguish between simple fractionation versus ingrowth processes during melting, as the cause for the ^{230}Th - ^{238}U and ^{231}Pa - ^{235}U disequilibrium in the melts, will be hindered. Consequently the conclusions about the physical parameters involved in melt generation and transport processes extracted from those isotopes will be equivocal.

[5] ^{226}Ra - ^{230}Th disequilibrium in mid-ocean ridge basalts (MORBs) is quite different from oceanic island basalts, not only because it is up to four times higher than ^{230}Th - ^{238}U disequilibrium, but also because the (^{226}Ra) excess is inversely correlated with the (^{230}Th) excess and with the extent of trace element depletion of the lavas (Figure 1) [Kelemen *et al.*, 1997a; Sims *et al.*, 2002, and references therein]. The large ^{226}Ra - ^{230}Th and ^{231}Pa - ^{235}U disequilibrium, and the positive correlation of the (^{231}Pa) excess with the (^{230}Th) excess that characterize mid-ocean ridge basalts can be explained by standard melting models; for example, dynamic melting with very short melt generation and extraction times [McKenzie, 2000], equilibrium porous flow [Spiegelman and Elliott, 1993], non-equilibrium melting processes [Qin, 1993] or a combination of these models. However, the inverse correlation of the (^{226}Ra) excess with the (^{230}Th) excess and with the lava trace element depletion cannot be explained by these models, and instead suggests that if the (^{231}Pa) and (^{230}Th) excesses are formed by deep seated melting processes, the (^{226}Ra) excess may be produced by melt/rock interaction in the shallow mantle [Kelemen *et al.*, 1997a]. For example, Jull *et al.* [2002] and Lundstrom [2000] explained the negative correlation of the activity ratios by a “two-porosity melting model” in which a slow moving melt that has traveled through reactive low porosity pathways mixes with a relatively fast moving melt that has been transported in unreactive

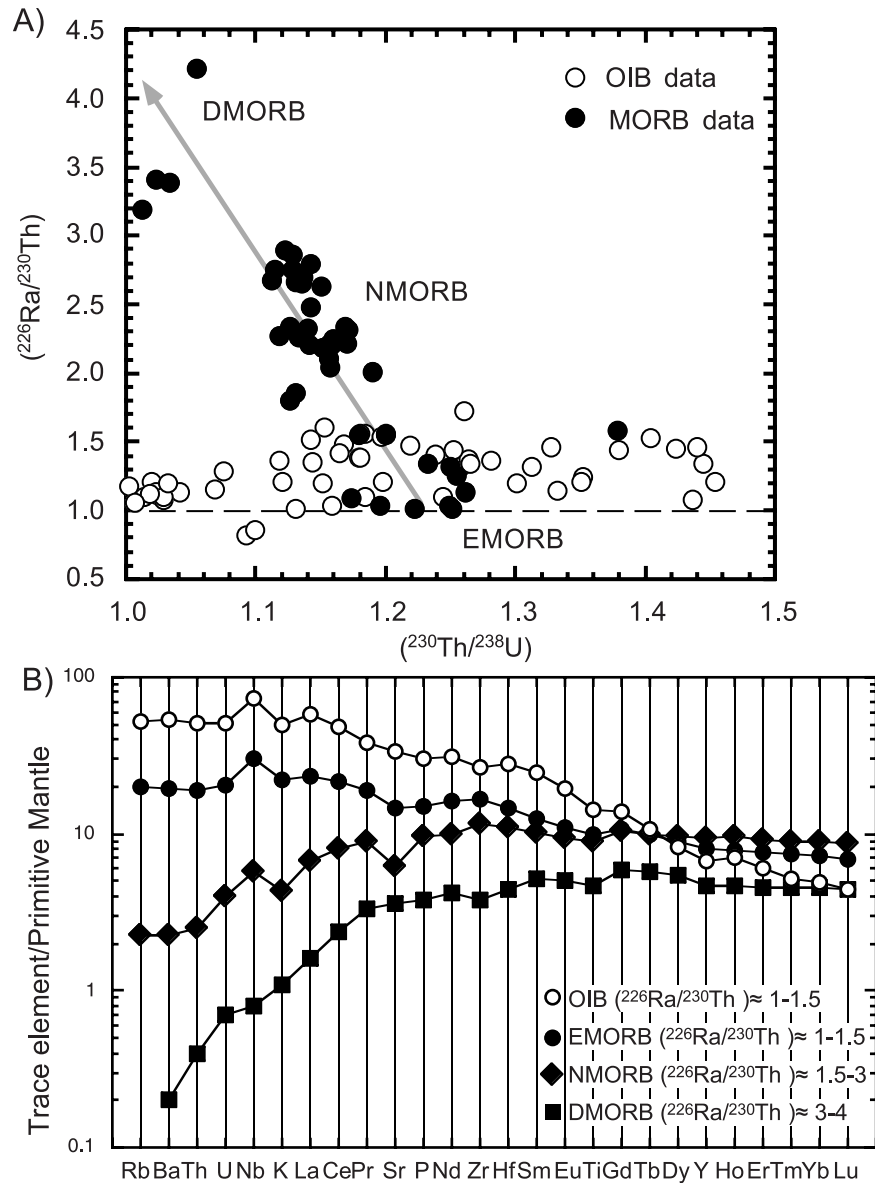


Figure 1. (a) $(^{226}\text{Ra})/(^{230}\text{Th})$ versus $(^{230}\text{Th})/(^{238}\text{U})$ activity ratios for mid-ocean ridge and oceanic island basalts. The data for MORBs represent a compilation for the Northern East Pacific Rise [Lundstrom *et al.*, 1999; Sims *et al.*, 2002; Volpe and Goldstein, 1993; Goldstein *et al.*, 1989, 1991, 1993]. Oceanic island basalts data were taken from Bourdon and Sims, [2003]. Note the inverse correlation between $(^{226}\text{Ra})/(^{230}\text{Th})$ and $(^{230}\text{Th})/(^{238}\text{U})$ activity ratios in the MORB data, where the melts with the highest $(^{226}\text{Ra})/(^{230}\text{Th})$ have the lowest $(^{230}\text{Th})/(^{238}\text{U})$ activity ratios [Kelemen *et al.*, 1997a; Sims *et al.*, 2002]. Furthermore, OIBs have similar ^{226}Ra and ^{230}Th activities and $(^{226}\text{Ra})/(^{230}\text{Th})$ ratios to EMORBs, but with a large range in $(^{230}\text{Th})/(^{238}\text{U})$ activity ratios. (b) Primitive mantle normalized trace element content of representative depleted, normal and enriched MORBs [Sims *et al.*, 2002] and OIBs [Sun and McDonough, 1989]. This figure further illustrates the inverse correlation between the $(^{226}\text{Ra})/(^{230}\text{Th})$ activity ratios and the trace element depletion of the oceanic basalts. Normalizing values from McDonough and Sun [1995].



high-porosity channels. Although the “two-porosity model” may explain the MORB data, the question that remains unanswered is whether the assumption used in all previous models, that the origin of ^{226}Ra - ^{230}Th disequilibrium is only produced during melt generation and transport in the mantle, is reasonable or not.

[6] Here we present an alternative process for the origin of the high (^{226}Ra) excess in oceanic basalts and for the inverse correlation of the (^{226}Ra) excess with the (^{230}Th) excess and with the extent of trace element depletion in MORB. We argue that (^{226}Ra) excess is produced by diffusive interaction of new batches of magma with cumulates crystallized at an earlier time from previous magmatic events. A major implication of our model is that inferences about mantle melting and melt transport in mid-ocean ridges and ocean islands drawn from (^{226}Ra)/(^{230}Th) activity ratios in basalts are equivocal.

2. Simple Diffusive Interaction Model of Oceanic Basalts With Cumulates in the Oceanic Lithosphere

[7] The objective of the simple model presented here is to determine the effect of diffusive chemical interaction on the ^{226}Ra - ^{230}Th - ^{238}U activity ratios during the percolation of oceanic basalts (MORBs and OIBs) through MORB cumulates. To illustrate this process, we present two simple cases where oceanic basalts, assumed initially to be in ^{226}Ra - ^{230}Th secular equilibrium, but with (^{230}Th)/(^{238}U) activity ratios representative of MORBs and OIBs, diffusively interact with (1) a zero age troctolite (plagioclase + olivine) and (2) an old (≈ 0.5 Ma) wehrlite (clinopyroxene + olivine). In both examples the cumulates crystallized at an earlier time from a normal MORB (NMORB) assumed initially to be in ^{226}Ra - ^{230}Th secular equilibrium, but with (^{230}Th)/(^{238}U) activity ratios representative of melts from the East Pacific Rise (see Table 1 for values and references).

[8] Geological, geophysical and petrological studies of ophiolites suggest that the crust-mantle transition zone beneath ocean ridges is one of the

possible areas where basalt-troctolite and basalt-wehrlite diffusive interaction may occur. This zone is a diffuse area formed by successive stages of basaltic melt injections, located between the underlying residual peridotite and the dominantly gabbroic crustal section. It is composed of dunites, chromitites, troctolites, wehrlites, pyroxenites and gabbroic sills of varying thickness. The composition of the rocks in this zone clearly show that they are cumulates formed by partial crystallization of MOR melts, and indicate that cumulates can form far below the level of magmatic neutral buoyancy [Nicolas and Prinzhofer, 1983; Nicolas *et al.*, 1988; Benn *et al.*, 1988; Boudier *et al.*, 1996; Kelemen *et al.*, 1997b]. Multichannel seismic studies of the crust-mantle transition zone show that this area is characterized by low seismic velocities, suggesting not only the presence of low melt fractions, a maximum of a couple of percent, but also inefficient heat removal from the transition zone [Dunn *et al.*, 2000, 2001; Dunn and Forsyth, 2003].

[9] The two examples presented here are simplified cases that allow us to evaluate different aspects of the diffusive interaction process between basalts and cumulates. Both cases assume that all the melts are initially in ^{226}Ra - ^{230}Th secular equilibrium. This assumption is the most conservative approach to evaluate whether the large (^{226}Ra) excess observed in oceanic basalts can be produced by melt-cumulate diffusive interaction. Moreover, the examples of cumulates used in our model are, although realistic, simple cases to evaluate the diffusive interaction between oceanic basalts and a single solid cumulate phase, such as plagioclase or clinopyroxene. Because olivine has no significant effect on the fractionation of ^{226}Ra - ^{230}Th - ^{238}U isotopes, the model assumes ^{226}Ra , ^{230}Th and ^{238}U diffusion only between melt and either clinopyroxene or plagioclase. Finally, the age of the cumulates plays a fundamental role in the results; we chose the two extreme examples that will produce the largest manifestation of the diffusive interaction on the (^{226}Ra) excess of the melt. A more general case would have been to consider a cumulate of gabbroic composition (clinopyroxene + plagioclase + olivine) and different ages, where



Table 1. Input Data^a

	NMORB	EMORB	DMORB	OIB	K^{Cpx}	Young cpx	Old cpx	K^{Plag}	Young plag	Old plag	D^{Cpx} [m ² /sec]	D^{Plag} [m ² /sec]
Th $\mu\text{g/g}$	0.194	1.477	0.026	6.709								
U $\mu\text{g/g}$	0.077	0.488	0.013	1.807								
Th/U	2.510	3.031	1.974	3.713								
(²³⁰ Th) dpm	6.759E-02	4.674E-01	9.90E-03	1.47E+00	2.1E-02	1.42E-03	1.03E-03	2.0E-03	1.352E-04	3.437E-05	3.2E-21	3.1E-21
(²³² Th) dpm	4.740E-02	3.610E-01	6.45E-03	1.64E+00	2.1E-02	9.95E-04	9.95E-04	2.0E-03	9.480E-05	9.480E-05	3.2E-21	3.1E-21
(²³⁸ U) dpm	5.728E-02	3.613E-01	9.90E-03	1.34E+00	1.8E-02	1.03E-03	1.03E-03	6.0E-04	3.437E-05	3.437E-05	2.1E-21	3.2E-21
(²³⁰ Ra) dpm	6.759E-02	4.674E-01	9.90E-03	1.47E+00	4.2E-05	2.84E-06	1.03E-03	4.86E-02	3.281E-03	3.437E-05	1.3E-17	6.9E-19
(²³⁸ U)/(²³² Th)	1.208	1.001	1.536	0.817		1.036	1.036		0.363	0.363		
(²³⁰ Th)/(²³² Th)	1.426	1.295	1.536	0.897		1.426	1.036		1.426	0.363		
(²³⁰ Th)/(²³⁸ U)	1.180	1.294	1.000	1.098		1.377	1.000		3.933	1.000		
(²²⁶ Ra)/(²³⁰ Th)	1.000	1.000	1.000	1.000		0.002	1.000		24.275	1.000		

^a Th and U concentrations for NMORB are averages of ICPMS data from Northern EPR (Donnelly, personal communication). Th and U concentrations of EMORB and DMORB are representative values from Siqueiros melts [Lundstrom et al., 1999]. Th and U concentrations of OIB are from *Claude-Ivanaj et al.* [2001]. ²²⁶Ra-²³⁰Th activities for all MORB and OIB are assumed to be in secular equilibrium initially. (²³⁰Th)/(²³⁸U) activity ratios are representative values for NMORB, EMORB and DMORB for the Northern EPR [Sims et al., 2002; Lundstrom et al., 1999; Volpe and Goldstein et al., 1989, 1991, 1993], and the value for the OIB is from the Azores [Claude-Ivanaj et al., 2001]. The K^{Cpx} and K^{Plag} are equilibrium melt-clinopyroxene partition coefficients from McDade et al. [submitted manuscript, 2003]. The K^{Cpx} is obtained using the K^{Cpx}/K^{Ba} \approx 0.7 from Blundy and Wood [2003] and the K^{Ba} \approx 6E-5 of Hauri et al. [1994]. The U, Th and Ra partition coefficients for plagioclase are not well known. The K^{Plag} is from J. D. Blundy and R. A. Brooker (Trace element partitioning during melting and crystallization of mafic rocks in the lower crust, manuscript submitted to *Contribution to Mineralogy and Petrology*, 2003), and the K^{Th} is obtained using the K^{Th}/K^{Ba} \approx 0.3 from Blundy and Wood [2003]. The K^{Ba} is from Cooper et al. [2001]. The D^{Cpx} and D^{Plag} are diffusion coefficients for clinopyroxene at 1200°C from Van Orman et al. [1998]. The D^{Cpx} , D^{Th} , D^{Ba} , D^{Ra} , D^{U} , D^{Th} , D^{Ba} , D^{Ra} were obtained using the model of Van Orman et al. [2001] (see text and caption to Figure 2). $\lambda^{238}\text{U}$ [dpm] = 2.951E-16, $\lambda^{230}\text{Th}$ [dpm] = 1.749E-11, $\lambda^{226}\text{Ra}$ [dpm] = 8.240E-10, $\lambda^{232}\text{Th}$ [dpm] = 9.414E-17. cpx = clinopyroxene; plag = plagioclase. “Young cpx” and “Young plag” represent \leq 100-year-old clinopyroxene and plagioclase cumulate respectively. “Old cpx” and “Old plag” represent \approx 0.5-Ma-old clinopyroxene and plagioclase cumulates. All cumulates are assumed to have crystallized from an NMORB.



diffusive exchange of isotopes takes place between coexisting plagioclase, clinopyroxene and melt. However, this requires a more complex model that takes into account interaction between a melt and two solid phases, and will be the focus of a future paper (Van Orman et al., manuscript in preparation, 2004). Yet, the two simple examples presented here bracket all the possible results produced by the most general case of melt-gabbro interaction.

[10] The model implemented here is a basic extension of the trace element diffusive fractionation model of *Van Orman et al.* [1998, 2002], and the derivation follows those papers. Essentially the model presented here considers diffusive interaction of mineral and melt without dissolution or crystallization. The solid is assumed to be composed of spherical grains of equal size, where grains are assumed to be homogeneous in composition when the melt-cumulate interaction begins. During the interaction, the interface between the solid and the melt is assumed to be in chemical equilibrium at all times; the mineral grains do not deform and the concentrations in the interior of the grains are controlled by simultaneous diffusion and isotopic decay. The concentration of ^{238}U , ^{230}Th and ^{226}Ra in the mineral phase can be represented by Fick's second law in spherical coordinates, modified to account for the decay of ^{238}U , ^{230}Th and ^{226}Ra :

$$\begin{aligned} \frac{\partial C_s^U}{\partial t} &= D_U(t) \left(\frac{\partial^2 C_s^U}{\partial r^2} + \frac{2}{r} \frac{\partial C_s^U}{\partial r} \right) - \lambda_U C_s^U \\ \frac{\partial C_s^{\text{Th}}}{\partial t} &= D_{\text{Th}}(t) \left(\frac{\partial^2 C_s^{\text{Th}}}{\partial r^2} + \frac{2}{r} \frac{\partial C_s^{\text{Th}}}{\partial r} \right) + \lambda_U C_s^U - \lambda_{\text{Th}} C_s^{\text{Th}} \quad (1) \\ \frac{\partial C_s^{\text{Ra}}}{\partial t} &= D_{\text{Ra}}(t) \left(\frac{\partial^2 C_s^{\text{Ra}}}{\partial r^2} + \frac{2}{r} \frac{\partial C_s^{\text{Ra}}}{\partial r} \right) + \lambda_{\text{Th}} C_s^{\text{Th}} - \lambda_{\text{Ra}} C_s^{\text{Ra}} \end{aligned}$$

where C_s^U , C_s^{Th} , C_s^{Ra} are the molar concentrations of ^{238}U , ^{230}Th and ^{226}Ra in the mineral grain at time t and radial distance r from the center of the grain, λ_U , λ_{Th} , λ_{Ra} are the decay constants, and D_U , D_{Th} , D_{Ra} are the diffusion coefficients in the solid phase.

[11] Mineral rims are assumed always to be in chemical equilibrium with the melt, so that:

$$C_s^i(R, t) = K_i C_m^i(t), \quad (2)$$

where K_i is the mineral-melt equilibrium partition coefficient, R is the radius of the mineral grain and C_m^i is the concentration of the isotope in the interacting melt.

[12] The variations of the total concentrations of ^{238}U , ^{230}Th and ^{226}Ra in the melt and mineral phase with time t are given by:

$$\begin{aligned} \frac{d}{dt} \left[\int_0^R 4\pi r^2 C_s^U dr + V_m C_m^U \right] &= -\lambda_U \left[\int_0^R 4\pi r^2 C_s^U dr + V_m C_m^U \right] \\ \frac{d}{dt} \left[\int_0^R 4\pi r^2 C_s^{\text{Th}} dr + V_m C_m^{\text{Th}} \right] &= -\lambda_{\text{Th}} \left[\int_0^R 4\pi r^2 C_s^{\text{Th}} dr + V_m C_m^{\text{Th}} \right] \\ &\quad + \lambda_U \left[\int_0^R 4\pi r^2 C_s^U dr + V_m C_m^U \right] \\ \frac{d}{dt} \left[\int_0^R 4\pi r^2 C_s^{\text{Ra}} dr + V_m C_m^{\text{Ra}} \right] &= -\lambda_{\text{Ra}} \left[\int_0^R 4\pi r^2 C_s^{\text{Ra}} dr + V_m C_m^{\text{Ra}} \right] \\ &\quad + \lambda_{\text{Th}} \left[\int_0^R 4\pi r^2 C_s^{\text{Th}} dr + V_m C_m^{\text{Th}} \right] \quad (3) \end{aligned}$$

where V_m is the volume of the melt and C_m^U , C_m^{Th} , C_m^{Ra} are the concentrations of ^{238}U , ^{230}Th and ^{226}Ra in the melt. These are mass balance equations that state that the change in the amount of isotope in the system is equal to that lost due to decay plus, for Ra and Th, the amount gained due to decay of the parent.

[13] The initial isotope concentrations in the mineral grain are different for clinopyroxene and plagioclase:

$$\begin{aligned} C_{\text{Cpx}}^U(r, 0) &= C_{\text{NMORB}}^U K_{\text{Cpx}}^{\text{Cpx}} \\ C_{\text{Cpx}}^{\text{Th}}(r, 0) &= C_{\text{Cpx}}^U (\lambda_U / \lambda_{\text{Th}}) \\ C_{\text{Cpx}}^{\text{Ra}}(r, 0) &= C_{\text{Cpx}}^U (\lambda_U / \lambda_{\text{Th}}) \quad (4) \\ C_{\text{Plag}}^U(r, 0) &= C_{\text{NMORB}}^U K_{\text{Plag}}^{\text{Plag}} \\ C_{\text{Plag}}^{\text{Th}}(r, 0) &= C_{\text{NMORB}}^{\text{Th}} K_{\text{Plag}}^{\text{Plag}} \\ C_{\text{Plag}}^{\text{Ra}}(r, 0) &= C_{\text{NMORB}}^{\text{Ra}} K_{\text{Plag}}^{\text{Plag}} \end{aligned}$$

C_{NMORB}^U is the initial concentration of ^{238}U in the NMORB from which the cumulate crystallized (Table 1). The first set of three equations represents the case of an old wehrlite, where the clinopyroxene is in secular equilibrium. The second set of equations represents the case of a young troctolite, where the activities of ^{238}U , ^{230}Th and ^{226}Ra in the plagioclase reflect equilibration with the melt. Both



cases assume that the cumulate crystallized from a NMORB initially in ^{226}Ra - ^{230}Th secular equilibrium, but with $(^{230}\text{Th})/(^{238}\text{U})$ activity ratios representative of melts from the East Pacific Rise.

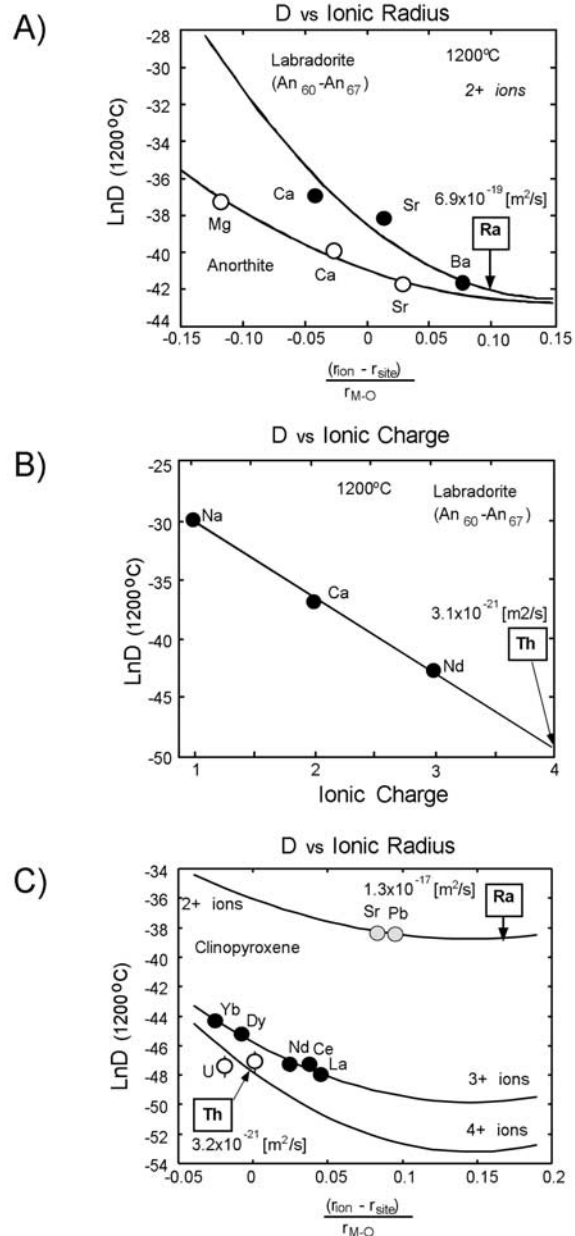
[14] The coupled set of equations (1)–(4) for each isotope is solved numerically using an implicit Crank-Nicolson finite difference scheme. We checked whether mass balance was achieved by comparing the amount of isotope present in the entire system (mineral + melt), at each time step, with the analytical solution to the isotope decay/production equation. In each case our numerical results agreed with the analytical solution to better than 2% relative.

[15] Although mineral-melt partition and diffusion coefficients for Th and U in clinopyroxene have been obtained experimentally [P. McDade, J. D. Blundy, and B. J. Wood (2003), Trace element partitioning on the Tinaquillo Lherzolite solidus at 1.5 GPa, manuscript submitted to *Physical Earth Planetary Interiors*, 2003, hereinafter referred to as McDade et al., submitted manuscript, 2003; Van Orman et al., 1998; Blundy and Wood, 2003, and references therein], they are missing for Ra in clinopyroxene, and are scarce or missing for U, Th and Ra in plagioclase [Cooper et al., 2001, 2003; Blundy and Wood, 2003, and references

therein]. Most values used for Ra partition coefficients have been calculated [Blundy and Wood, 2003; Cooper et al., 2001, 2003] using the theoretical elastic strain model of Blundy and Wood [1994]. To obtain diffusion coefficients that have not been determined experimentally, we used the lattice elastic strain model of Van Orman et al. [2001], which relates the diffusion coefficient to the ionic radius and charge of the diffusing ion (Figure 2).

[16] We performed a series of model runs using the parameter values listed in Table 1. Melts were

Figure 2. (a) $\ln D_{1200^\circ\text{C}}$ versus $(r_{\text{ion}} - r_{\text{site}})/r_{\text{M-O}}$ for alkaline earth elements in plagioclase (labradorite: Ca, Behrens et al. [1990]; Ba, Cherniak [2002a]; Sr, Cherniak and Watson [1994]; anorthite: Mg, Ca and Sr, La Tourrette and Wasserburg [1998]). r_{ion} is the radius of the ion, r_{site} is the ideal site radius, and $r_{\text{M-O}}$ is the average cation-anion bond length. The curves are fits of the lattice elastic strain model of Van Orman et al. [2001] to the experimental data, with similar Ra diffusion coefficients calculated from either the labradorite or anorthite data. (b) $\ln D_{1200^\circ\text{C}}$ versus ionic charge for Na, Ca and Nd in labradorite plagioclase (Na and Ca, Behrens et al. [1990]; Nd, Cherniak [2002b]). These three ions have similar ionic radii and the defined line is the best fit to the experimental data used to constrain the Th diffusivity in plagioclase. (c) $\ln D_{1200^\circ\text{C}}$ versus $(r_{\text{ion}} - r_{\text{site}})/r_{\text{M-O}}$ for U, Th, Sr, Pb and rare earth elements in clinopyroxene (REE, Van Orman et al. [2001]; U and Th, Van Orman et al. [1998]; Sr, Sneeringer et al. [1984]; Pb, Cherniak [1998]). The curves are best fits lattice elastic strain model of Van Orman et al. [2001] to the experimental data.





assumed to interact with two different cumulates, both of which crystallized from an NMORB: a “young” troctolite ($\ll 100$ years) that has retained its original ^{226}Ra - ^{230}Th - ^{238}U activity ratios, and an “old” wehrlite (≈ 0.5 Ma) that has reached ^{226}Ra - ^{230}Th - ^{238}U secular equilibrium before melt-rock interaction begins. We assume that the troctolite and the wehrlite were composed of 50% olivine and 50% plagioclase or 50% clinopyroxene respectively. As mentioned above, previous studies of the crust-mantle transition zone constrain the grain size of the crystal phases to 0.5–1 mm [Boudier *et al.*, 1996], the melt to rock ratio to 0.5 – 1% and the temperature to approximately 1200°C [Dunn *et al.*, 2000]. We assume that the temperature remained constant at 1200°C, consistent with the inferred inefficient heat removal from the transition zone [Dunn *et al.*, 2000]. The initial melt compositions used are representative values for depleted (DMORB), normal (NMORB) and enriched (EMORB) melts from the East Pacific Rise [Lundstrom *et al.*, 1999; Sims *et al.*, 2002; Volpe and Goldstein, 1993; Goldstein *et al.*, 1989, 1991, 1993; K. Donnelly, personal communication, 2003] and for oceanic island basalts [Claude-Ivanaj *et al.*, 2001], where we assumed that all the melts have ^{230}Th - ^{238}U disequilibrium as reported in the literature, but with ^{226}Ra - ^{230}Th activity ratios in secular equilibrium (Table 1).

3. Results and Discussion

[17] The results of our model are shown in Figures 3, 4a, 4b, and Table 2. Our results clearly demonstrate that diffusive interaction during percolation of oceanic basalts through transition zone cumulates may produce significant changes in the activity of ^{226}Ra without extensive modification of the initial ^{230}Th and ^{238}U activities in the melt. Thus during melt-cumulate interaction, the $(^{226}\text{Ra})/(^{230}\text{Th})$ ratio in the melt radically diverges from that initially produced during mantle melting, while the $(^{230}\text{Th})/(^{238}\text{U})$ ratio remains almost unchanged. Fundamentally, our results show the role that the different diffusion coefficients of the isotopes play on the ^{226}Ra - ^{230}Th disequilibrium during melt-cumulate interaction. ^{226}Ra diffusion is approximately 100 to 10000

times faster than ^{230}Th and ^{238}U in plagioclase and clinopyroxene respectively, while ^{230}Th and ^{238}U diffuse at almost the same rate in each mineral (Figure 2, Table 1) [Van Orman *et al.*, 1998]. More importantly, this simple model not only reproduces the ^{226}Ra - ^{230}Th - ^{238}U activities and ratios observed in MORBs, but also replicates the observed inverse correlation of the (^{226}Ra) excess with the (^{230}Th) excess and with the trace element depletion in mid-ocean ridge basalts (Figures 4a and 4b).

3.1. Effect of Composition

[18] We present 6 cases where normal (NMORB), depleted (DMORB) and enriched (EMORB-OIB) melts interact with a young plagioclase cumulate and with an old clinopyroxene cumulate, both crystallized at an earlier time from a normal MORB. In Figure 3 we show that the larger the chemical disequilibrium between the percolating melt and the NMORB cumulate, the more susceptible the melt will be to diffusive interaction. Thus depleted and enriched basalts interacting with a young plagioclase cumulate will experience the largest modification of their ^{226}Ra and ^{230}Th activities and ratios (Figures 3a and 3c), while NMORBs will undergo small isotopic modifications (Figure 3b). Depleted and enriched basalts have ^{226}Ra and ^{230}Th activities lower and higher, respectively, than those of the NMORB in equilibrium with the cumulate. Therefore ^{226}Ra and ^{230}Th will diffuse from the cumulate into the depleted melt, and from the enriched melt into the cumulate, in attempting to reach equilibrium. Because ^{226}Ra diffuses much faster than ^{230}Th , the resulting $(^{226}\text{Ra})/(^{230}\text{Th})$ ratios will increase in the DMORB to values higher than 1, but will decrease in the enriched melts to values less than 1 during the interaction. When an NMORB is interacting with a young plagioclase cumulate, the only cause of modification of the $(^{226}\text{Ra})/(^{230}\text{Th})$ ratio in the melt is the decay of unsupported ^{226}Ra in the plagioclase. The decreasing $(^{226}\text{Ra})/(^{230}\text{Th})$ ratio in the cumulate produces an associated decrease of $(^{226}\text{Ra})/(^{230}\text{Th})$ ratio in the melt, due to the diffusion of ^{226}Ra from the melt to the plagioclase cumulate. In summary, melts interacting with a plagioclase cumulate will have $(^{226}\text{Ra})/(^{230}\text{Th})$ ratios up to 4 in DMORBs,

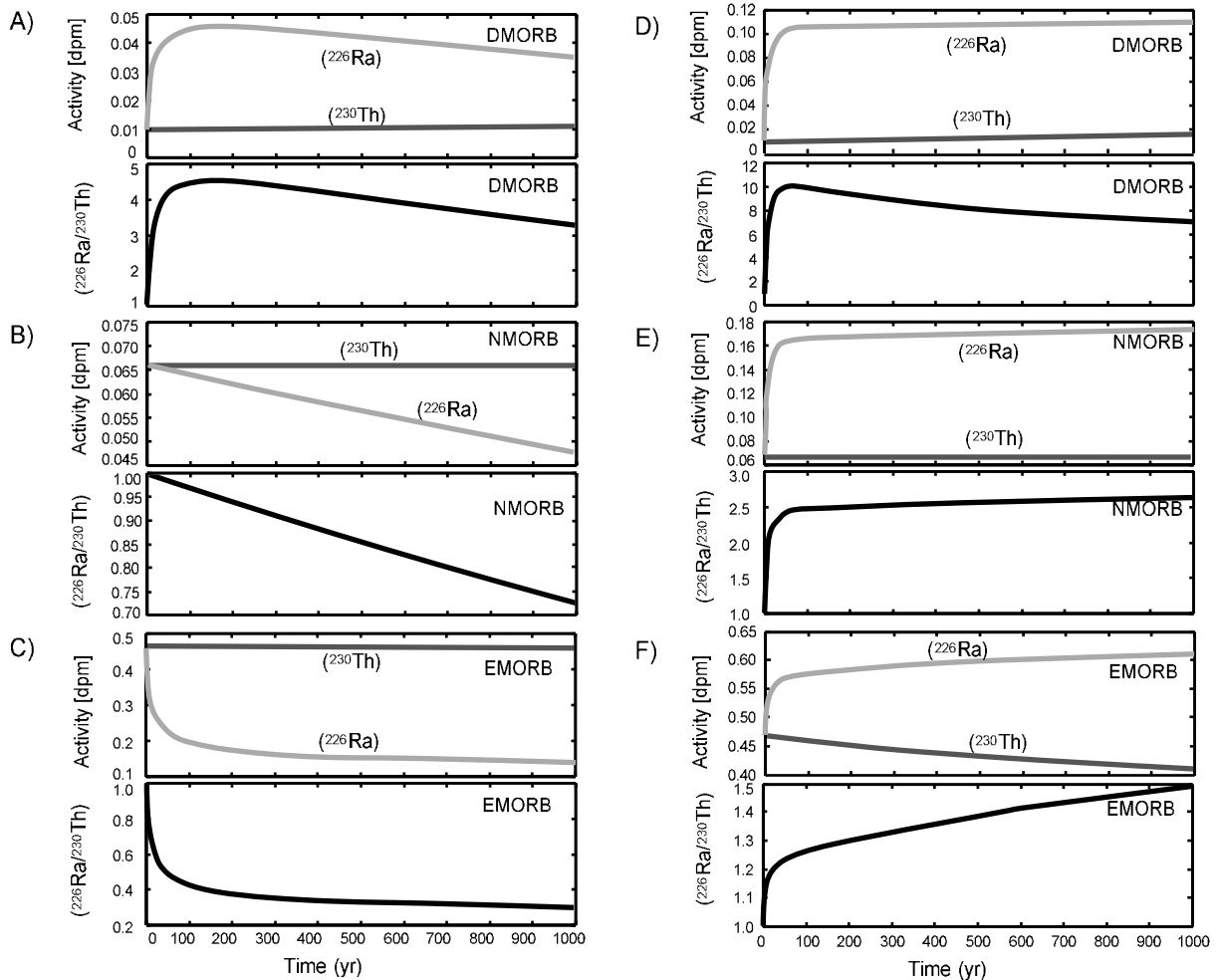


Figure 3. Calculated results of diffusive interaction between oceanic basalts and cumulates previously crystallized from an NMORB in the crust-mantle transition zone. The results are displayed as ^{226}Ra and ^{230}Th activities and $(^{226}\text{Ra})/(^{230}\text{Th})$ ratios versus interaction time. We present 6 cases where normal (NMORB), depleted (DMORB) and enriched (EMORB/OIB) melts interact with a young (<100 yr) troctolite cumulate (cases A, B and C) and with an old ($\approx 0.5\text{-Ma}$) clinopyroxene cumulate (cases D, E and F). For the examples presented here, we assumed the troctolite and the wehrlite formed by 50% olivine and 50% plagioclase or 50% clinopyroxene respectively, 0.5 mm for the grain size of the crystal phases, 0.5% for the melt to rock ratio, and 1200°C for the temperature. The input and output data of the model are shown in Tables 1 and 2, respectively.

close to 1 in NMORBs and lower than 1 in enriched melts.

[19] The interaction of basalts with an old clinopyroxene cumulate is quite different from that of a young plagioclase cumulate. In an old ($\approx 0.5\text{Ma}$) clinopyroxene cumulate the ^{226}Ra - ^{230}Th - ^{238}U activities will be in secular equilibrium; that is, the activities of these three isotopes will be the same. Accordingly, the activities of ^{226}Ra and ^{230}Th in old clinopyroxenes are high because their initial ^{238}U activities are significant. Because the clino-

pyroxene-melt partition coefficient for Ra is so small, the melt in equilibrium with an old clinopyroxene-cumulate will generally have higher ^{226}Ra activity than any of the depleted, normal or enriched melts. Hence during the interaction of these melts with the cumulate ^{226}Ra will diffuse from the cumulate to the melt regardless of the melt composition (Figures 3d, 3e, and 3f). However, the increase in ^{226}Ra for each interacting melt composition is inversely proportional to the initial ^{226}Ra activity (i.e., degree of enrichment) in the interacting melt. For instance, in our examples the increase of ^{226}Ra

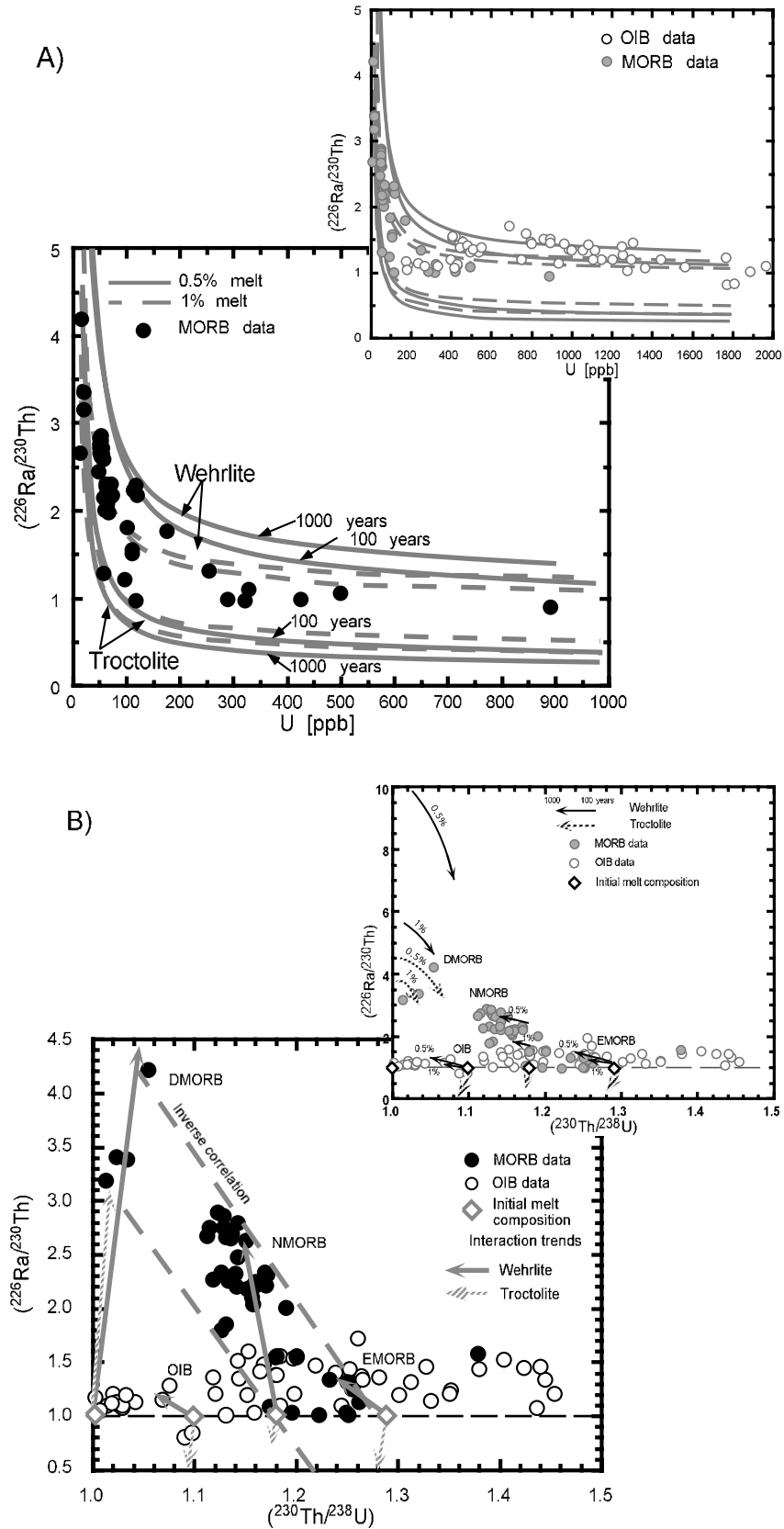


Figure 4.



Table 2a. Model Results: Melt Interacting With Young Plagioclase Cumulate From NMORB^a

	100 yr interaction			300 yr interaction			1000 yr interaction		
	U (ppb)	^(230Th) / ^(238U)	^(226Ra) / ^(230Th)	U (ppb)	^(230Th) / ^(238U)	^(226Ra) / ^(230Th)	U (ppb)	^(230Th) / ^(238U)	^(226Ra) / ^(230Th)
	<i>Melt Fraction 0.5%</i>								
DMORB	13.30	1.011	4.5091	13.40	1.030	4.367	13.59	1.068	3.262
	28.27	1.090	2.155	28.34	1.100	2.081	28.48	1.110	1.621
	51.54	1.146	1.282	51.58	1.147	1.213	51.65	1.150	0.969
NMORB	77.28	1.180	0.947	77.28	1.179	0.877	77.28	1.178	0.712
	98.79	1.199	0.805	98.76	1.198	0.734	98.70	1.194	0.602
	197.5	1.246	0.560	197.3	1.243	0.486	197.0	1.236	0.410
EMORB	483.8	1.292	0.421	483.2	1.287	0.345	482.0	1.278	0.301
	987.3	1.316	0.375	986.0	1.311	0.298	983.3	1.301	0.264
OIB	1,791	1.096	0.360	1,789	1.092	0.283	1,784	1.085	0.252
	<i>Melt Fraction 1%</i>								
DMORB	13.28	1.005	3.78	13.33	1.015	3.89	13.42	1.034	3.047
	28.25	1.088	1.911	28.29	1.091	1.918	28.36	1.097	1.553
	51.53	1.145	1.223	51.55	1.146	1.184	51.59	1.147	0.982
NMORB	77.28	1.180	0.960	77.28	1.179	0.901	77.28	1.178	0.761
	98.80	1.200	0.848	98.78	1.199	0.781	98.75	1.196	0.667
	197.6	1.247	0.655	197.5	1.245	0.573	197.3	1.241	0.503
EMORB	484.0	1.293	0.547	483.7	1.290	0.456	583.1	1.285	0.410
	987.7	1.317	0.510	987.0	1.314	0.417	985.7	1.308	0.379
OIB	1,792	1.097	0.499	1,790	1.095	0.404	1,788	1.091	0.369

^a Tables 2a and 2b shows the output results of the melt-cumulate diffusive interaction model for melts ranging in composition from DMORBs to OIBs. While the values from DMORB, NMORB, EMORB and OIB are from published papers (see Table 1), the intermediate values are interpolation between those extreme compositions.

Figure 4. Comparison of data from oceanic basalts with the results of our diffusive interaction model. The data for MORB represent a compilation for the Northern East Pacific Rise [Lundstrom *et al.*, 1999; Sims *et al.*, 2002; Volpe and Goldstein, 1993; Goldstein *et al.*, 1989, 1991, 1993]. OIB data were taken from a compilation by Bourdon and Sims [2003], and unpublished data of Bourdon and Turner (in preparation, 2003). (a) ^(226Ra)/^(230Th) activity ratios versus U content for oceanic basalts. The models represent melts interacting with young troctolite and old wehrlite cumulates as shown in Figure 3 and Table 2. Solid and dashed lines correspond to melt-rock ratios of 0.5 and 1% respectively. Also, for each case we show two extreme melt-rock interaction times: 100 and 1000 years. This diagram demonstrates the influence that the trace element enrichment of the melts has on the final result. The most enriched lavas (high U content) have ^(226Ra)/^(230Th) activity ratios closer to or lower than 1, while the most depleted lavas have ^(226Ra)/^(230Th) ratios much higher than 1. The inset shows an extension of the same figure including the OIB data. Our two simplified models shown here bracket the data for oceanic basalt, suggesting that plagioclase ± clinopyroxene ± olivine cumulates may be responsible for the ^(226Ra)/^(230Th) ratios observed in MORBs and OIBs. (b) ^(226Ra)/^(230Th) versus ^(230Th)/^(238U) activity ratios for oceanic basalts. The arrows represent schematic trends of the diffusive interaction processes between melt and troctolite or wehrlite, where the initial ^(226Ra)/^(230Th) ratios of the melts undergo large changes without significant modifications of their ^(230Th)/^(238U) ratios. ^(226Ra)/^(230Th) ratios substantially increase in depleted melts (DMORB) and slightly increase or even decrease in enriched melts (EMORB and OIB) during diffusive interaction processes, producing the inverse correlation observed in ocean-ridge basalts. The inset is the same diagram at a different scale, where we show the actual results of our model presented in Table 2. Arrows represent the evolution of ^(226Ra)/^(230Th) and ^(230Th)/^(238U) activity ratios in the melt with increasing interaction time. Each arrow corresponds to a range in time from 100 (arrow tail) to 1000 (arrow head) years interaction. Diamonds represent the initial composition of melts (Table 1). The number near the arrows represents the percent of melt. Note that in the cases of melt-troctolite interaction for OIB, N- and EMORBs the arrows for 0.5% and 1% melt overlap and are not distinguishable. Also, note that our diffusive interaction model is able to reproduce the ^(226Ra)/^(230Th) ratios lower than 1 as measured in some OIBs. See text for details.



Table 2b. Model Results: Melt Interacting With Old Clinopyroxene-Cumulate From NMORB

	100 yr interaction			300 yr interaction			1000 yr interaction		
	U (ppb)	$(^{230}\text{Th})/$ (^{238}U)	$(^{226}\text{Ra})/$ (^{230}Th)	U (ppb)	$(^{230}\text{Th})/$ (^{238}U)	$(^{226}\text{Ra})/$ (^{230}Th)	U (ppb)	$(^{230}\text{Th})/$ (^{238}U)	$(^{226}\text{Ra})/$ (^{230}Th)
<i>Melt Fraction 0.5%</i>									
DMORB	14.15	1.026	9.893	15.91	1.058	8.671	19.44	1.080	7.023
	28.91	1.090	5.121	30.26	1.094	4.959	32.97	1.091	4.625
	51.88	1.142	3.217	52.59	1.134	3.254	54.02	1.118	3.270
NMORB	77.28	1.174	2.465	77.29	1.162	2.540	77.31	1.140	2.641
	98.51	1.192	2.143	97.93	1.179	2.226	96.76	1.155	2.353
	196.0	1.238	1.579	192.7	1.221	1.666	186.1	1.193	1.816
EMORB	478.5	1.283	1.259	467.4	1.264	1.341	445.1	1.234	1.493
	975.4	1.307	1.151	950.5	1.287	1.230	900.5	1.256	1.380
OIB	1,769	1.089	1.117	1,722	1.073	1.194	1,630	1.049	1.343
<i>Melt Fraction 1%</i>									
DMORB	13.73	1.015	5.65	14.69	1.036	5.259	16.65	1.056	4.592
	28.60	1.089	3.102	29.33	1.091	3.067	30.84	1.091	2.954
	51.72	1.143	2.125	52.10	1.139	2.153	52.91	1.130	2.170
NMORB	77.28	1.177	1.745	77.29	1.170	1.786	77.31	1.157	1.836
	98.65	1.196	1.583	98.34	1.188	1.627	97.71	1.174	1.687
	196.7	1.243	1.301	195.0	1.233	1.348	191.3	1.216	1.421
EMORB	481.1	1.288	1.142	475.2	1.277	1.188	462.8	1.259	1.265
	981.3	1.312	1.088	967.9	1.301	1.134	940.3	1.282	1.212
OIB	1,780	1.093	1.071	1,755	1.084	1.117	1,703	1.070	1.193

activity in the melts ranges from a factor of 10 to 2.5 to 1.3 in DMORB, NMORB and EMORB-OIB respectively. In contrast to ^{226}Ra , ^{230}Th will diffuse from the cumulate to the depleted melt or from the enriched melt to the cumulate, and it will not be significantly modified in the normal MORB (Figures 3d, 3e, and 3f). The final result of diffusive interaction between melts and clinopyroxene cumulates is that EMORBS will evolve toward $(^{226}\text{Ra})/(^{230}\text{Th})$ ratios close to 1, DMORBs will reach values higher than 4, and NMORBs will attain values intermediate between these extremes.

[20] The $(^{230}\text{Th})/(^{238}\text{U})$ ratios of the melt will remain mostly unchanged whether the interaction is with a plagioclase or clinopyroxene cumulate (Table 2a), as expected due to the small and similar diffusion coefficients for ^{238}U and ^{230}Th in each mineral. Depleted melts will be the most affected, with a 3% change in their $(^{230}\text{Th})/(^{238}\text{U})$ ratios for a 400% change in their $(^{226}\text{Ra})/(^{230}\text{Th})$ ratios. Thus while $(^{230}\text{Th})/(^{238}\text{U})$ ratios remains mostly unaffected, the $(^{226}\text{Ra})/(^{230}\text{Th})$ ratios will significantly increase in DMORBs, stay close to secular equilibrium or even decrease in EMORBs-OIBs, and attain values between those two extremes in

NMORBs, creating the observed inverse correlations in mid-ocean ridge basalts (Figures 4a and 4b).

[21] Comparable diffusive processes may also explain why most oceanic island basalts (OIBs) have lower $(^{226}\text{Ra})/(^{230}\text{Th})$ ratios than depleted and normal MORBs (Figure 4). Essentially, OIBs contain similar or higher ^{226}Ra , ^{230}Th , and ^{238}U activities and ratios than EMORBs (*Bourdon and Sims, 2003*). As a result, the interaction of OIBs with cumulates in the oceanic lithosphere may produce low $(^{226}\text{Ra})/(^{230}\text{Th})$ at any range of $(^{230}\text{Th})/(^{238}\text{U})$ ratios. For example, Figure 4b shows that our diffusive interaction process may explain the $(^{226}\text{Ra})/(^{230}\text{Th})$ lower than 1 observed in some OIBs [*Claude-Ivanaj et al., 2001*]. Hence previous inferences drawn from $(^{226}\text{Ra})/(^{230}\text{Th})$ systematics about the physical processes involved in the generation and transport of oceanic basalts are at best equivocal.

3.2. Effect of the Cumulate Age

[22] The examples of cumulates used in our model are, although realistic, simplified cases to evaluate the effect of young plagioclase and old clinopyroxene during diffusive interaction with basalts. The age of these cumulates plays a fundamental



role in the results. Young plagioclase cumulates have $(^{226}\text{Ra})/(^{230}\text{Th})$ ratios higher than 1, but the high ^{226}Ra concentration in the plagioclase is unsupported by its low ^{230}Th content. Consequently, the $(^{226}\text{Ra})/(^{230}\text{Th})$ and $(^{230}\text{Th})/(^{238}\text{U})$ ratios in the plagioclase will decrease toward secular equilibrium over time, with the ^{226}Ra activity eventually equaling that of ^{230}Th (Table 1). Therefore an old troctolite will not create high $(^{226}\text{Ra})/(^{230}\text{Th})$ ratios in a diffusively interacting melt. Interaction of melts with an old troctolite can only lead to $(^{226}\text{Ra})/(^{230}\text{Th})$ ratios that are less than or equal to 1. In the same way, a young clinopyroxene cumulate has $(^{226}\text{Ra})/(^{230}\text{Th})$ ratios less than 1 (Table 1); thus, a young wehrlite will not create high $(^{226}\text{Ra})/(^{230}\text{Th})$ ratios in an interacting melt either. As the wehrlite gets older, the $(^{226}\text{Ra})/(^{230}\text{Th})$ ratio will quickly ($\approx 8,000$ years) approach secular equilibrium, increasing the ^{226}Ra activity in the clinopyroxene to equal that of ^{230}Th . The increase in ^{226}Ra with time makes the wehrlite suitable for producing $(^{226}\text{Ra})/(^{230}\text{Th})$ ratio >1 in the melt by diffusive interaction. As a simple rule, the larger the proportion of clinopyroxene to plagioclase, the older the gabbroic cumulate will have to be to produce high $(^{226}\text{Ra})/(^{230}\text{Th})$ ratios in the interacting melt and vice versa. Undoubtedly real cases are more complicated than those presented in this paper, with cumulates of different ages formed by different proportions of clinopyroxene, plagioclase and olivine. However, the results of the two simplified cases shown here bracket the published oceanic basalt data (Figure 4a), suggesting that plagioclase \pm clinopyroxene \pm olivine cumulates may be responsible for the $(^{226}\text{Ra})/(^{230}\text{Th})$ ratios observed in MORBs and OIBs.

3.3. Effect of the Interaction Time

[23] As shown in the previous section, time is an important factor in the cumulate isotopic composition; therefore, we have to consider the role that the interaction time plays in the resulting $(^{226}\text{Ra})/(^{230}\text{Th})$ ratio of the melt. Two main competing factors control the activities and ratios during diffusive interaction: (1) the diffusion coefficients and (2) the decay rates of the different isotopes. At short interaction times the isotopic ratios are

principally controlled by the diffusion rates, but as time progresses the effects of decay and production of isotopes become more important. Figure 3 show the changes in the ^{226}Ra - ^{230}Th activities and ratios with increasing interaction time from 0 to 1,000 years. Most examples show that the main changes in the activity ratios of the melt occur in the first 100 years. In the case of young or old plagioclase cumulates, the longer the time of interaction beyond 100 years, the lower will be the $(^{226}\text{Ra})/(^{230}\text{Th})$ ratios of the melt (Figure 3a). The decrease of the activity ratio in the melt with time is mainly due to the decay of unsupported ^{226}Ra activity in the plagioclase cumulate. In contrast, in the case of a clinopyroxene cumulate in secular equilibrium, the ^{226}Ra activity in the mineral is supported by its ^{230}Th activity. As a result, the $(^{226}\text{Ra})/(^{230}\text{Th})$ ratios of the melt will tend to increase with time for the EMORB and decrease for the DMORB (Figure 3b). The main cause of the change in activity ratio in the melts with time is due to the difference in ^{226}Ra and ^{230}Th concentration between the interacting melt and the melt in equilibrium with the cumulate. As mentioned above, in every case considered here ^{226}Ra will diffuse from the clinopyroxene to the melt. In contrast, ^{230}Th will diffuse either from the cumulate to the depleted melt or from the enriched melt to the cumulate. Most of the ^{226}Ra within the clinopyroxene diffuses out within the first 50 years of interaction; afterward there is only a slow leakage of ^{226}Ra into the melt as it is produced by decay of ^{230}Th . As a result, in DMORB, the $(^{226}\text{Ra})/(^{230}\text{Th})$ ratio increases rapidly in the first ~ 50 years, then begins to decrease as the rate of release of ^{226}Ra into the melt falls below that of ^{230}Th . In the case of a normal MORB, ^{230}Th is not significantly modified with time, but ^{226}Ra slowly increases in the melt due to continuous ingrowth of ^{226}Ra in the clinopyroxene and diffusion into the melt. In EMORB, ^{230}Th steadily decreases in the melt as it diffuses into the cumulate, while ^{226}Ra increases, leading to a continuous increase in $(^{226}\text{Ra})/(^{230}\text{Th})$. If the clinopyroxene cumulate is young, the $(^{226}\text{Ra})/(^{230}\text{Th})$ ratio of the melt will increase as the interaction time increases, because ^{230}Th in the clinopyroxene has time to decay and produce more ^{226}Ra , which will ultimately diffuse into the melt.



[24] From the previous examples, it is clear that the time of interaction between melts and cumulates is a fundamental variable that we have to constrain. The time the melt remains in contact with the cumulate will depend on the volume of the melt-rock interaction zone, its porosity, the spreading rate and the thickness of the oceanic crust. Assuming that the area of interaction beneath mid-ocean ridges is 3 km deep and 20 km wide, with 0.5% porosity, an overlying crustal thickness of approximately 6 km, and a spreading rate of 100 km/My, the residence time of melt in the crust-mantle transition zone is 500 years. Therefore we believe that a range from 0 to 1000 years reasonably constrains the interaction time.

3.4. Effect of Grain Size

[25] The grain size in the cumulate is another important variable that affects the results of our model. Essentially, increasing the grain size is equivalent to reducing the surface area over which the diffusive interaction takes place. Thus the result of increasing grain size will be comparable to decreasing the melt-cumulate interaction time. Increasing the plagioclase grain size will require a longer interaction time to achieve the same degree of diffusive exchange; however, with longer interaction times the unsupported ^{226}Ra activity in the plagioclase decays, resulting in lower $(^{226}\text{Ra})/(^{230}\text{Th})$ ratios in the melts. In contrast, in a young or old clinopyroxene cumulate ^{226}Ra is supported by the ^{230}Th content; therefore, longer interaction times will allow ^{230}Th to decay to ^{226}Ra , which will subsequently diffuse into the melt generating high $(^{226}\text{Ra})/(^{230}\text{Th})$ ratios.

3.5. Effect of the Melt/Cumulate Ratio

[26] An additional variable to take into account in our model is the fraction of melt interacting with the cumulate. Our results indicate that the larger the melt-filled porosity in the cumulate, the smaller the effect of diffusive interaction on the melt. As the melt fraction increases, the ^{226}Ra - ^{230}Th activities and ratios of the original melt will change a smaller amount during the melt-cumulate interaction (Figures 4a and 4b, Table 2). On the basis of seismic data, there is some constraint on the porosity

in the crust-mantle transition zone. Multi-channel seismic experiments in the EPR [Dunn *et al.*, 2000, 2001; Dunn and Forsyth, 2003] constrain the porosity in this zone to a couple of percent at most. Therefore the melt to cumulate ratio will always be very small and the effect of diffusive interaction in the crust-mantle transition zone may thus have a large influence on the $(^{226}\text{Ra})/(^{230}\text{Th})$ ratios of the melt. It is important to remark that although the fraction of melt in the crust-mantle transition zone is small, it represents a large fraction of the total volume of melt below the ridge axis.

3.6. Effect of Plagioclase or Clinopyroxene Undersaturation

[27] Although in the model presented here we assumed that the interacting melt is saturated with plagioclase and clinopyroxene, a simple mass balance calculation illustrates that undersaturation and partial dissolution of these phases into the melt will have a negligible effect on the ^{226}Ra and ^{230}Th ratios of that melt. For example, if a melt dissolves an amount of clinopyroxene or plagioclase comparable to its own mass, assuming crystallization of an equivalent amount of olivine to maintain the heat balance, the isotopic composition of the melt will change slightly. The most affected melt is the DMORB, due to its low ^{226}Ra and ^{230}Th concentration, where the resulting $(^{226}\text{Ra})/(^{230}\text{Th})$ ratios will at most change by 9%. This variation is insignificant compared to the 400 to 1000% change of $(^{226}\text{Ra})/(^{230}\text{Th})$ ratios in DMORBs during diffusive interaction with plagioclase or clinopyroxene cumulates respectively. Essentially, this can be explained as a result of the small melt-rock ratio in the interaction zone. For a cumulate with 2% porosity and 0.5 mm grain size, dissolution of a mass of clinopyroxene or plagioclase equal to the mass of the melt involves only the outermost ~ 10 microns of the crystal; meanwhile diffusive exchange of ^{226}Ra may take place over the entire volume of the crystal.

3.7. Simple Mass Balance Consideration

[28] In this paper we have shown that diffusive interaction of small-degree melts with clinopyroxene- or plagioclase-bearing cumulates can lead to



large ^{226}Ra excesses in the melts. But can this process plausibly explain ^{226}Ra excesses in all MORB? To answer this question we must evaluate whether there is enough ^{226}Ra in the cumulates to account for excess ^{226}Ra in the oceanic basalts. If Ra is treated as a non-radiogenic trace element then the answer is certainly no; because U, Th and Ra are all highly incompatible, only a mass of cumulates more than an order of magnitude greater than erupted MORB would contain enough ^{226}Ra to account for the ^{226}Ra excess in MORB. Such a large reservoir of cumulates is implausible. It is therefore necessary to consider in situ production of ^{226}Ra in the cumulates, and to ask whether the production rate is large enough to account for the outflux of ^{226}Ra at mid-ocean ridges.

[29] Most of the ^{226}Ra production in the cumulates occurs within clinopyroxene, and because the Ra solubility in clinopyroxene is very low nearly all of the ^{226}Ra produced is potentially available for delivery to the melt. If the cumulate-melt interaction zone has a volume of 60 km^3 ($20\text{ km} \times 3\text{ km} \times 1\text{ km}$) and contains 30% clinopyroxene, the mass of clinopyroxene is approximately 5.8×10^{16} grams. The ^{238}U activity in clinopyroxene crystallized from an NMORB is approximately 1.0×10^{-3} disintegrations per minute per gram (Table 1), meaning that the rate of ^{226}Ra production in the cumulate is about 3×10^{19} atoms per year, or somewhat higher if the clinopyroxene has excess ^{230}Th .

[30] For an average spreading rate of 5 cm/yr and erupted basalt thickness of 2 km, the mass of basalt that must pass through the cumulate zone is about 2.7×10^{11} grams per year. Assuming that the basalt is NMORB with an initial ($^{226}\text{Ra}/^{230}\text{Th}$) activity ratio of unity and a final activity ratio of 2.0 after melt-cumulate interaction, approximately 2×10^{19} atoms of ^{226}Ra must be absorbed by the basalt per year. This is similar to the rate of ^{226}Ra production in the cumulate, and it therefore appears possible for the cumulate to supply a sufficient flux of ^{226}Ra to explain the excesses observed in erupted MORB.

4. Conclusions

[31] The simple model presented in this paper demonstrates the effect that melt-cumulate diffu-

sive interaction processes have on the ^{226}Ra - ^{230}Th disequilibrium of oceanic basalts. We showed that such processes may control not only the ($^{226}\text{Ra}/^{230}\text{Th}$) ratios observed in mid-ocean ridge basalts, but also their inverse correlation with the ($^{230}\text{Th}/^{238}\text{U}$) activity ratios and with the extent of trace element depletion. Moreover, our model may explain the observed difference in ^{226}Ra - ^{230}Th disequilibrium between MORBs and OIBs without invoking changes in the mantle melting conditions. Hence the inference drawn from ($^{226}\text{Ra}/^{230}\text{Th}$) activity ratios about mantle melting and melt transport in mid-ocean ridges and ocean islands are equivocal.

Acknowledgment

[32] We wish to acknowledge Aaron Pietruszka, Tim Elliott, Peter Kelemen, Roberta Rudnick and Willian White for comments and suggestions that considerably improved the manuscript. We benefited greatly from the discussions with Craig Lundstrom, Erik Hauri, Bernard Bourdon, Ken Sims and Mathew Jull. Both authors contributed equally to this work. This work was supported by NSF grant EAR-0207136 to Alberto Saal and grant EAR-0337125 to James Van Orman.

References

- Allègre, C. J., and M. Condomines (1982), Basalt genesis and mantle structure studied through Th-isotopic geochemistry, *Nature*, 299, 21–24.
- Behrens, H., W. Johannes, and H. Schmalzried (1990), On the mechanisms of cation diffusion processes in ternary feldspars, *Phys. Chem. Miner.*, 17, 62–78.
- Benn, K., A. Nicolas, and I. Reuber (1988), Mantle-crust transition zone and origin of wehrlitic magmas: Evidence from the Oman ophiolite, *Tectonophysics*, 151, 75–85.
- Blundy, J. D., and B. J. Wood (1994), Prediction of crystal-melt partition coefficients from elastic moduli, *Nature*, 372, 452–454.
- Blundy, J. D., and B. J. Wood (2003), Mineral-melt partitioning of Uranium, Thorium and their daughters, in *Uranium-Series Geochemistry, Rev. Mineral. Geochem.*, vol. 52, edited by B. Bourdon et al., pp. 59–118, Mineral. Soc. of Am., Washington, D. C.
- Boudier, F., A. Nicolas, and I. Benoît (1996), Magma chambers in the Oman ophiolite: Fed from the top and the bottom, *Earth Planet. Sci. Lett.*, 144, 239–250.
- Bourdon, B., and K. W. Sims (2003), U-series constraints on intraplate basaltic magmatism, in *Uranium-Series Geochemistry, Rev. Mineral. Geochem.*, vol. 52, edited by B. Bourdon et al., pp. 215–253, Mineral. Soc. Am., Washington, D. C.
- Cherniak, D. J. (1998), Pb diffusion in clinopyroxene, *Chem. Geol.*, 150, 105–117.



- Cherniak, D. J. (2002a), Ba diffusion in feldspar, *Geochim. Cosmochim. Acta*, *66*, 1641–1651.
- Cherniak, D. J. (2002b), REE diffusion in feldspar, *Chem. Geol.*, *193*, 25–41.
- Cherniak, D. J., and E. B. Watson (1994), A study of strontium diffusion in plagioclase using Rutherford Backscattering spectroscopy, *Geochim. Cosmochim. Acta*, *58*, 5179–5190.
- Claude-Ivanaj, C., J. L. Joron, and C. J. Allègre (2001), ^{238}U - ^{230}Th - ^{226}Ra fractionation in historical lavas from the Azores: Long-lived source heterogeneity vs. metasomatism fingerprints, *Chem. Geol.*, *176*, 295–310.
- Cooper, K. M., M. R. Reid, M. T. Murrell, and D. A. Clague (2001), Crystal and magma residence at Kilauea volcano, Hawaii: ^{230}Th - ^{226}Ra dating of the 1955 east rift eruption, *Earth Planet. Sci. Lett.*, *184*, 703–718.
- Cooper, K. M., S. J. Goldstein, K. W. Sims, and M. T. Murrell (2003), Uranium-series chronology of the Gorda Ridge volcanism: New evidence from the 1996 eruption, *Earth Planet. Sci. Lett.*, *206*, 459–475.
- Dunn, R. A., and D. W. Forsyth (2003), Imaging the transition between the region of mantle melt generation and the crustal magma chamber beneath the southern East Pacific Rise with short-period Love waves, *J. Geophys. Res.*, *108*(B7), 2352, doi:10.1029/2002JB002217.
- Dunn, R. A., D. R. Toomey, and S. C. Solomon (2000), Three-dimensional seismic structure and physical properties of the crust and shallow mantle beneath the East Pacific Rise at 9°30' N, *J. Geophys. Res.*, *105*, 23,537–23,555.
- Dunn, R. A., D. R. Toomey, R. S. Detrick, and W. S. Wilcock (2001), Continuous mantle melt supply beneath an overlapping spreading center on the East Pacific Rise, *Science*, *291*, 1955–1958.
- Goldstein, S. J., M. T. Murrell, and D. E. Janecky (1989), Th and U isotopic systematic of basalts from the Juan de Fuca and Gorda Ridges by mass spectrometry, *Earth Planet. Sci. Lett.*, *96*, 134–146.
- Goldstein, S. J., M. T. Murrell, D. E. Janecky, J. R. Delaney, and D. A. Clague (1991), Geochronology and petrogenesis of MORB from the Juan de Fuca and Gorda Ridges by ^{238}U - ^{230}Th disequilibrium, *Earth Planet. Sci. Lett.*, *107*, 25–41.
- Goldstein, S. J., M. T. Murrell, and R. W. Williams (1993), ^{231}Pa and ^{230}Th chronology of mid-ocean ridge basalts, *Earth Planet. Sci. Lett.*, *115*, 151–159.
- Hauri, E. H., T. P. Wagner, and T. L. Grove (1994), Experimental and natural partitioning of Th, U, Pb and other trace elements between garnet, clinopyroxene and basaltic melts, *Chem. Geol.*, *117*, 149–166.
- Iwamori, H. (1994), ^{238}U - ^{230}Th - ^{226}Ra and ^{235}U - ^{231}Pa disequilibria produced by mantle melting with porous and channel flows, *Earth Planet. Sci. Lett.*, *125*, 1–16.
- Jull, M., P. B. Kelemen, and K. W. Sims (2002), Consequences of diffuse and channeled porous melt migration on Uranium series, *Geochim. Cosmochim. Acta*, *66*, 4133–4148.
- Kelemen, P. B., G. Hirth, N. Shimizu, M. Spiegelman, and H. J. Dick (1997a), A review of melt migration processes in the adiabatically upwelling mantle beneath oceanic spreading ridges, *Philos. Trans. R. Soc. London*, *355*, 283–318.
- Kelemen, P. B., K. Koga, and N. Shimizu (1997b), Geochemistry of gabbro sills in the crust-mantle transition zone of the Oman ophiolite: Implications for the origin of the oceanic lower crust, *Earth Planet. Sci. Lett.*, *146*, 475–488.
- La Tourrette, T., and G. J. Wasserburg (1998), Mg diffusion in anorthite: Implications for the formation of early solar system planetesimals, *Earth Planet. Sci. Lett.*, *158*, 91–108.
- Lundstrom, C. C. (2000), Model of U-series disequilibria generation in MORB; the effects of two scales of melt porosity, *Phys. Earth Planet. Int.*, *121*, 189–204.
- Lundstrom, C. C. (2003), Uranium-series disequilibria in mid-ocean ridge basalts: Observations and models of basalt genesis, in *Uranium-Series Geochemistry*, *Rev. Mineral. Geochem.*, vol. 52, edited by B. Bourdon et al., pp. 175–212, Mineral. Soc. of Am., Washington, D. C.
- Lundstrom, C. C., D. E. Sampson, M. R. Perfit, J. B. Gill, and Q. Williams (1999), Insights into mid-ocean ridge basalt petrogenesis; U-series disequilibria from the Siqueiros Transform, Lamont Seamounts, and East Pacific Rise, *J. Geophys. Res.*, *104*, 13,035–13,048.
- McDonough, W. F., and S.-S. Sun (1995), The composition of the Earth, *Chem. Geol.*, *120*, 223–253.
- McKenzie, D. (1985), ^{230}Th - ^{238}U disequilibrium and the melting processes beneath ridge axes, *Earth Planet. Sci. Lett.*, *72*, 149–157.
- McKenzie, D. (2000), Constraints on melt generation and transport from U-series activity ratios, *Chem. Geol.*, *162*, 81–94.
- Nicolas, A., and A. Prinzhofer (1983), Cumulative or residual origin for the transition zone in ophiolites: Structural evidence, *J. Petrol.*, *24*, 188–206.
- Nicolas, A., I. Reuber, and K. Benn (1988), A new magma chamber model based on structural studies in the Oman ophiolite, *Tectonophysics*, *151*, 87–105.
- Qin, Z. (1993), Dynamics of melt generation beneath mid-ocean ridge axes; theoretical analysis based on ^{238}U - ^{230}Th - ^{226}Ra and ^{235}U - ^{231}Pa disequilibria, *Geochim. Cosmochim. Acta*, *57*, 1629–1634.
- Sims, K. W., D. J. DePaolo, M. T. Murrell, W. S. Baldrige, S. J. Goldstein, and D. Clague (1995), Mechanism of magma generation beneath Hawaii and mid-ocean ridges: Uranium/thorium and samarium/neodymium isotopic evidence, *Science*, *267*, 508–512.
- Sims, K. W., D. J. DePaolo, M. T. Murrell, W. S. Baldrige, S. J. Goldstein, D. Clague, and M. Jull (1999), Porosity of the melting zone and variations in the solid mantle upwelling rate beneath Hawaii: Inferences from ^{238}U - ^{230}Th - ^{226}Ra and ^{235}U - ^{231}Pa disequilibria, *Geochim. Cosmochim. Acta*, *63*, 4119–4138.
- Sims, K. W., et al. (2002), Chemical and isotopic constraints on the generation and transport of magma beneath the East Pacific Rise, *Geochim. Cosmochim. Acta*, *66*, 3481–3504.
- Sneeringer, M., S. R. Hart, and N. Shimizu (1984), Strontium and samarium diffusion in diopside, *Geochim. Cosmochim. Acta*, *48*, 1589–1608.
- Spiegelman, M. (2000), UserCalc: A Web-based uranium series calculator for magma migration problems, *Geochim. Geophys. Geosyst.*, *1*, Paper number 1999GC000030.



- Spiegelman, M., and T. Elliott (1993), Consequences of melt transport for U-series disequilibrium in young lavas, *Earth Planet. Sci. Lett.*, *118*, 1–20.
- Sun, S.-S., and W. F. McDonough (1989), Chemical and isotopic systematics of oceanic basalts: Implications for mantle composition and processes, in *Magmatism in the Ocean Basins*, edited by A. D. Saunders and M. J. Norris, *Geol. Soc. Spec. Publ.*, *42*.
- Van Orman, J. A., T. L. Grove, and N. Shimizu (1998), Uranium and thorium diffusion in diopside, *Earth Planet. Sci. Lett.*, *160*, 505–519.
- Van Orman, J. A., T. L. Grove, and N. Shimizu (2001), Rare earth element diffusion in diopside: Influence of temperature, pressure, and ionic radius, and an elastic model for diffusion in silicates, *Contrib. Mineral. Petrol.*, *141*, 687–703.
- Van Orman, J. A., T. L. Grove, and N. Shimizu (2002), Diffusive fractionation of trace elements during production and transport of melt in Earth's upper mantle, *Earth Planet. Sci. Lett.*, *198*, 93–112.
- Volpe, A. M., and S. J. Goldstein (1993), ²²⁶Ra-²³⁰Th disequilibrium in axial and off-axis mid-ocean ridge basalts, *Geochem. Cosmochim. Acta*, *57*, 1233–1241.
- Williams, R. W., and J. B. Gill (1989), Effects of partial melting on the ²³⁸U decay series, *Geochem. Cosmochim. Acta*, *53*, 1607–1619.